

# Recent constraints on the parton distributions in the proton and the measurement of $\alpha_S$ from ATLAS and CMS

M. R. Sutton

*Department of Physics and Astronomy, University of Sussex, Falmer,  
Brighton BN1 9QH, United Kingdom*

On behalf of the  
ATLAS and CMS Collaborations

Recent results on cross sections sensitive to the parton distribution functions (PDFs) within the proton from the ATLAS and CMS Collaborations are presented. The potential impact on the inclusion of these data in fits to the PDFs is discussed. Recent results from fits including the data from jet, or vector boson production from the ATLAS and CMS experiments are discussed.

## 1 Introduction

The LHC <sup>1</sup> is an exemplary machine for the study of perturbative QCD. All processes at the LHC take place between quarks and gluons so, given sufficient understanding of the hard interaction, any physics process could in principle be used to constrain the parton density functions (PDFs) within the proton. Precise knowledge of these PDFs is an essential prerequisite for the identification of any possible signature from physics beyond the Standard Model.

During Run 1, the LHC performed extremely well, allowing both the ATLAS <sup>2</sup> and CMS <sup>3</sup> collaborations to collect proton-proton data samples in excess of  $25 \text{ fb}^{-1}$  per experiment. These large samples are allowing the development of an increasingly large and diverse portfolio of precision analyses from each collaboration that are useful for constraining the parton distributions in the proton in a kinematic regime beyond any previously available.

The data presented in this article were collected during 2010 and 2011 and represent only about one fifth of these Run 1 data sets. In addition, the remaining  $20 \text{ fb}^{-1}$  of data from the 8 TeV running in 2012 available from each collaboration, are currently being analysed. Results from these analyses of the 2012 data will be published in the near future.

When performing fits for the proton parton distributions, different physics processes provide information on the different parton initial states. The very precise HERA inclusive DIS data typically only tightly constrain the parton distributions at lower- $x$ , and are sensitive to the gluon at Next-to-leading order (NLO) through scaling violations <sup>4</sup>. The LHC cross section on the other hand, with two target hadrons, is sensitive to the gluon distribution and the strong coupling already at leading order (LO) for processes including dijet or  $t\bar{t}$  production, and to the valence quarks at higher  $E_T$ , whereas Electroweak boson production, is sensitive both to the valence and sea quark distributions.

For LHC processes, the cross section is generally only calculable after the numerical integration over the phase space to cancel the infra-red and collinear divergences, so fast convolution techniques are required, such as those implemented by the fastNLO <sup>5</sup> and APPLgrid <sup>6</sup> projects.

## 2 Jet production and the gluon distribution

Fits to the proton PDFs <sup>7,8,9,10</sup> using only data from experiments with lower momentum transfer than available at the LHC typically have large uncertainties for the LHC kinematic region, notably at high- $x$  <sup>11</sup>. This is most apparent for the gluon distribution, where the difference between the central fits from the different groups are sometimes larger than the uncertainties on

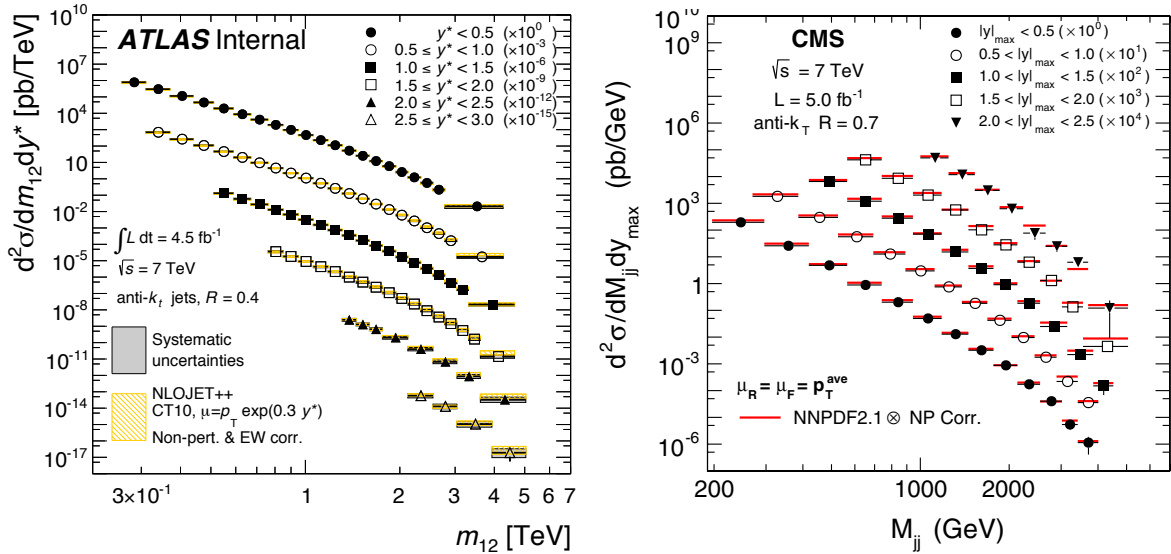


Figure 1 – The ATLAS (left) and CMS (right) dijet mass from the 2011 dijet data

the individual PDFs themselves. This gives rise to a significant uncertainty on the predictions of LHC cross sections, such as in Higgs, or  $t\bar{t}$  production<sup>11</sup>.

For jet production at the LHC, at all but the highest  $p_T$ , the cross section is dominated by quark-gluon scattering and so the data should provide a significant additional constraint on the gluon distribution with respect to that from the HERA or fixed target data alone.

Fig. 1 shows the new dijet data from both the ATLAS<sup>12</sup> and CMS<sup>13</sup> collaborations in different regions of dijet rapidity, spanning a range of 200 GeV to 5 TeV in dijet mass. The data themselves are reasonably well described over eight orders of magnitude in variation of the cross section and a mass range from around 250 GeV to 5 TeV – somewhat of a triumph for perturbative QCD.

In Fig.2 can be seen the ratio of theory over data for each of the six rapidity ranges seen in Fig. 1 for the ATLAS data. This illustrates that the systematic uncertainties, which are dominated by the Jet Energy Scale, are typically between 5-10% for central rapidities, and increase at higher rapidities and higher masses where the data is in any case, more statistically limited. In all cases, the experimental uncertainties are already comparable to the theoretical uncertainties. The data are shown compared to the NLO QCD predictions using the CT10<sup>7</sup>, and HERAPDF fits<sup>10</sup>, and also the atlas epJet13 fit<sup>14</sup> which used the 2.76 and 7 TeV jet data from 2010. There appears to be a possible tendency for the CT10 fit to be slightly harder, with the fit to the ATLAS 2010 data, describing the shape better at high masses. The gluon-gluon terms in the full next-to-next to leading order (NNLO) calculation have recently been calculated<sup>15</sup> and show approximately a 25% contribution, although the contribution to the cross section in the LHC kinematic region of the gluon-gluon term is small and predominantly at low  $E_T$ .

Quantitative analysis on the level of agreement of the cross section with the predictions of the different PDFs<sup>12</sup> illustrate that most of the PDFs fits reasonable well, whereas the ABM11<sup>9</sup> with a softer gluon contribution, is somewhat disfavoured.

### 3 QCD analysis

Both ATLAS and CMS have presented fits to their inclusive jet data – the ATLAS fit<sup>14</sup> using both the 7 and 2.76 TeV from 2010 and CMS<sup>16</sup> using their more recent 2011 inclusive data<sup>17</sup>.

Both Collaborations use a similar parameterisation with a more flexible gluon distribution. Sum rules are used to constrain many of the parameters, and in both the ATLAS and CMS fits

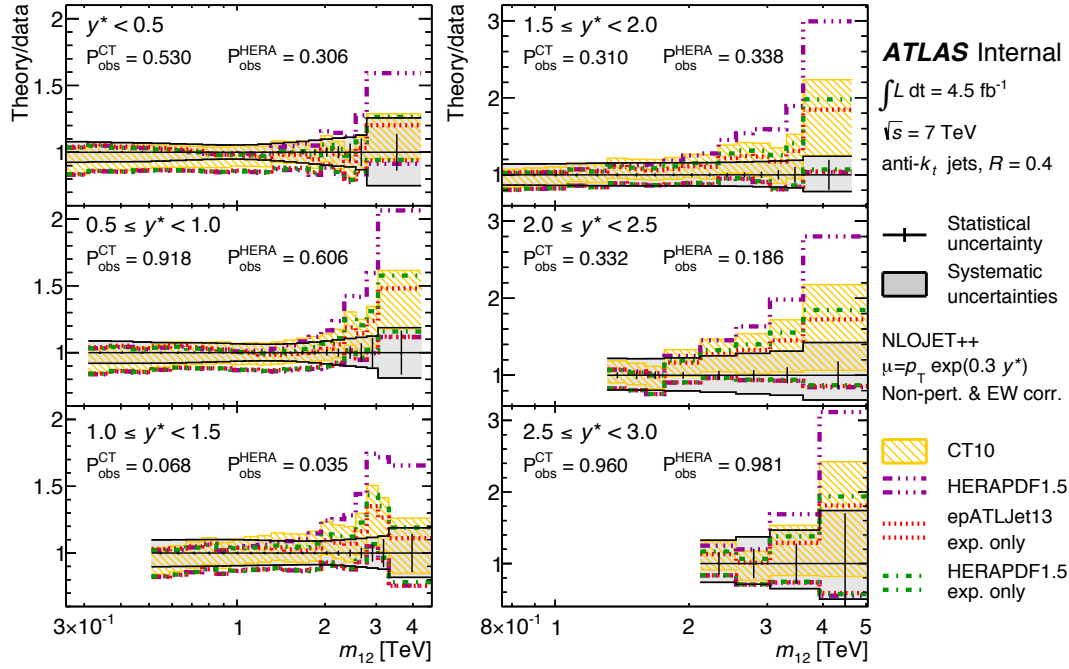


Figure 2 – The ratio of the theory prediction to the ATLAS jjet data for different PDFs.

the strange distribution is constrained to be strictly proportional to the d-type sea, resulting in a 13 parameter fit. Both collaborations also include the HERA DIS data in their fits, as well as their own data which are reproduced using either fastNLO or APPLgrid.

The resulting gluon distribution from the CMS collaboration can be seen in Fig. 3. This also shows the fit resulting from just the HERA DIS data shown as the hatched band. For the fits from both ATLAS and CMS the gluon distribution is harder than that obtained from HERA data alone, with a slightly different shape and with a significantly reduced uncertainty at higher- $x$ . Most noticeable is the reduction in the uncertainty at high- $x$  at a scale of  $10^4$  GeV<sup>2</sup>.

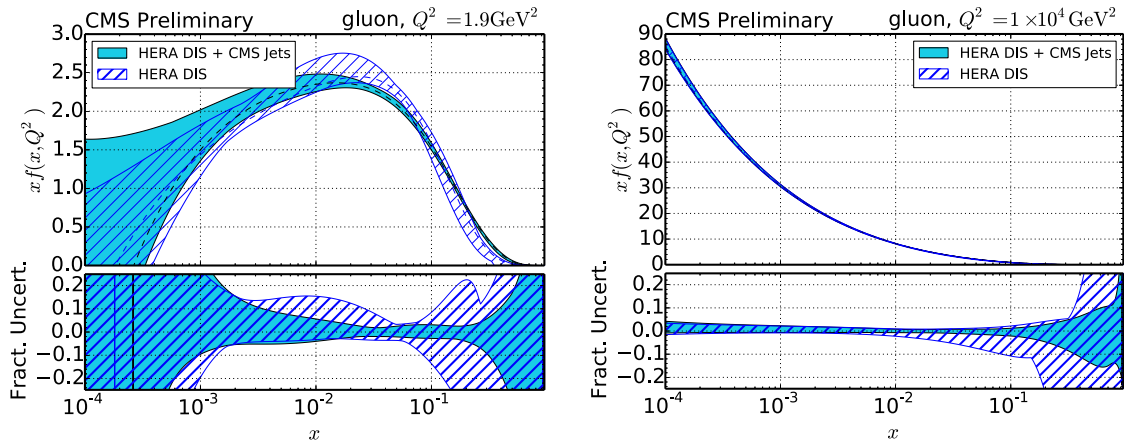


Figure 3 – The gluon distribution from the CMS fit; (left) at the starting scale of  $1.9 \text{ GeV}^2$  and (right) at a scale of  $10^4 \text{ GeV}^2$

The direct  $t\bar{t}$  production cross section is also sensitive to the gluon distribution and measurements have been performed by both ATLAS<sup>18</sup> and CMS<sup>19</sup>. Comparisons of the ATLAS data with theory at NLO suggest that the data may be better described by the HERAPDF rather than the CT10 PDF, which has a slightly harder gluon distribution from the inclusion of the Tevatron jet data.

## 4 The strong coupling

The top production data are also sensitive to the strong coupling, or conversely, to the mass top quark itself. By constraining the top mass to a value,  $173.2 \pm 1.4$  GeV, the CMS collaboration has extracted the strong coupling using an NNLO fit<sup>19</sup>, where the result is  $0.1151^{+0.0033}_{-0.0032}$ , consistent with the world average.

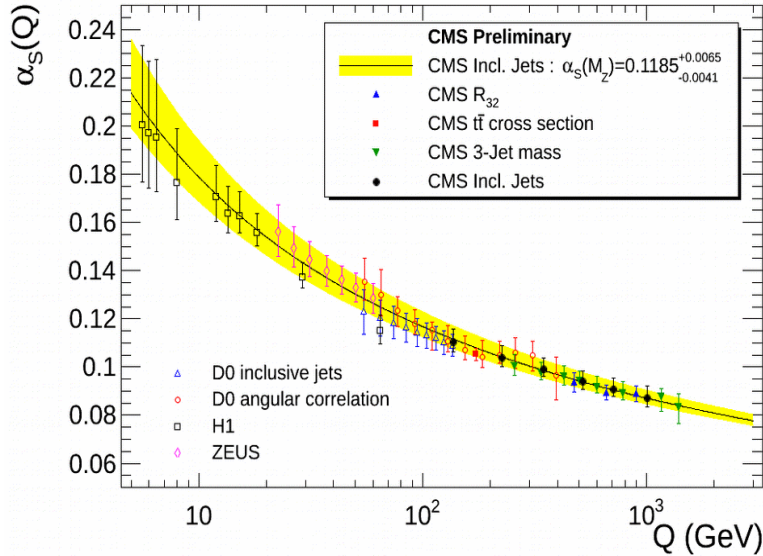


Figure 4 – The strong coupling measured using the CMS data compared to measurements from HERA and the Tevatron.

In addition, CMS has also extracted the strong coupling from several jet measurements. Fig. 4 shows the strong coupling extracted using from these jet data for the ratio of 3-to-2 jet production<sup>20</sup>, the 3-jet mass<sup>21</sup>, and inclusive jet production<sup>17</sup>. In addition, the value from the fit using the top data is also shown. The running of the strong coupling can clearly be seen up to scales nearly an order of magnitude higher than measured previously at either HERA<sup>22,23,24</sup> or the Tevatron<sup>25,26,27</sup>.

The value of the strong coupling measured using the CMS inclusive jet data<sup>16</sup> is  $0.1185^{+0.0065}_{-0.0041}$  again consistent with the world average.

## 5 Photon production

A measuring that has the potential to sample the hard subprocess directly is that of prompt photon production. As in the case of jet production, the dominant production mechanism is quark-gluon scattering. This process has the potential to also constrain the gluon distribution, although in this case it is also more sensitive to the contribution from  $u-g$  scattering because of the larger charge on the  $u$ -quark. A sensitivity study from ATLAS<sup>28</sup> using the data on inclusive direct photon production<sup>29</sup> suggests that the softer gluon distribution from the ABM11 PDF is able to describe the shape of the cross-section better, but with a lower normalisation. Taking into consideration the systematic uncertainties, all the PDFs fit the data reasonably well, with the harder gluon distribution from CT10 being less favoured.

## 6 Heavy Electroweak boson production

With the production of heavy Electroweak bosons, it is possible to better constrain the valence and sea quark distributions. Data from the ATLAS<sup>30</sup> and CMS<sup>31</sup> collaborations on Drell-Yan production are becoming rather precise, particularly in the region of the  $Z$  resonance, and suggest that the NNLO cross section with a number PDFs fitted at NNLO tend to lie somewhat below the data for central rapidities.

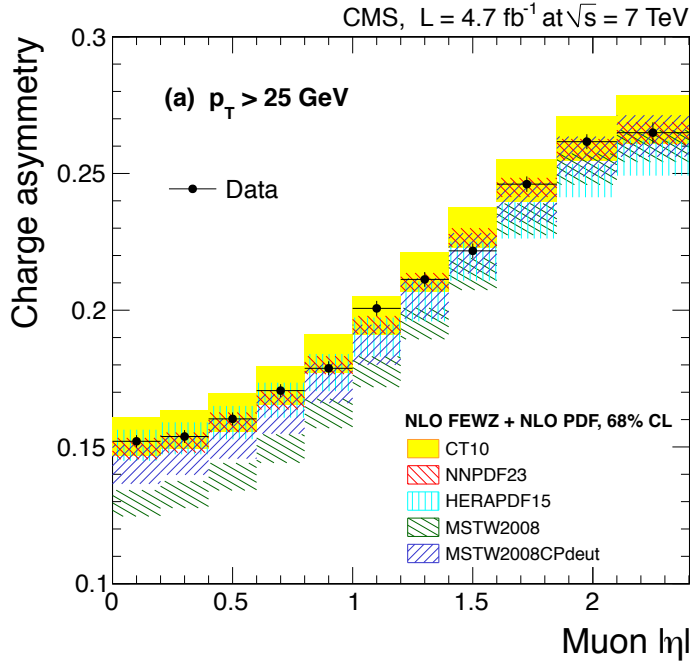


Figure 5 – The CMS Electroweak charged  $W$  asymmetry data from 2011.

The charge asymmetry of the  $W^+$  and  $W^-$  data when taken in combination has the potential to largely cancel the contribution from the gluon for which the uncertainty can be large. If the approximate equivalence of quark and anti-quark sea can be assumed then much of the sea quark contribution will also vanish, allowing these processes to provide valuable information on the  $u$  and  $d$ -valence quark distributions. An additional benefit of taking the charge asymmetry is the potential to also cancel many of the correlated experimental systematic uncertainties.

In practice the  $W$  kinematics cannot be measured, but fortunately the lepton asymmetry remains sensitive to the valence quark distributions.

The charge asymmetry data from CMS<sup>32</sup> is shown in Fig. 5 compared to calculations at NLO. The theoretical uncertainties are typically larger than the experimental uncertainties at NLO. Some discrimination between the data is already visible - particularly for the default MSTW2008 fit<sup>8</sup>, which lies below the data for small muon pseudorapidities. This is somewhat improved with the updated MSTW2008 fit including data from deuteron scattering, but still predicts a slightly smaller asymmetry. Note that the HERPDF predicts too small an asymmetry at larger rapidities. Although the  $W$  cross section is known to NNLO, differences between the PDFs are still apparent.

## 7 Heavy Electroweak boson production with charm

Events with a  $W$  candidate and a charm quark in the final state are directly sensitive to the strange quark density. Recent results from the ATLAS<sup>33</sup> and CMS<sup>34</sup> collaborations measure the differential cross section for measuring a  $W$  in conjunction with either a fully reconstructed charmed hadron, or by identifying a charmed jet by the presence of a soft lepton within a jet itself.

The differential cross section for the rapidity of leptons from the  $W$  decay for charmed jet events from both ATLAS and CMS is shown in Fig. 6. Here the general trend of the predictions suggests that the NNPDF2.3coll fit<sup>35</sup> predicts the highest overall cross section and MSTW2008 the lowest, although the level of agreement with these predictions is different between the two measurements. The ATLAS and CMS measurements are not strictly comparable – for the ATLAS measurement the lepton selection is  $p_T^{\text{lepton}} > 40$  GeV whereas for the CMS measurement it is  $p_T^{\text{lepton}} > 35$  GeV – although there still may be a tendency for the ATLAS cross section to

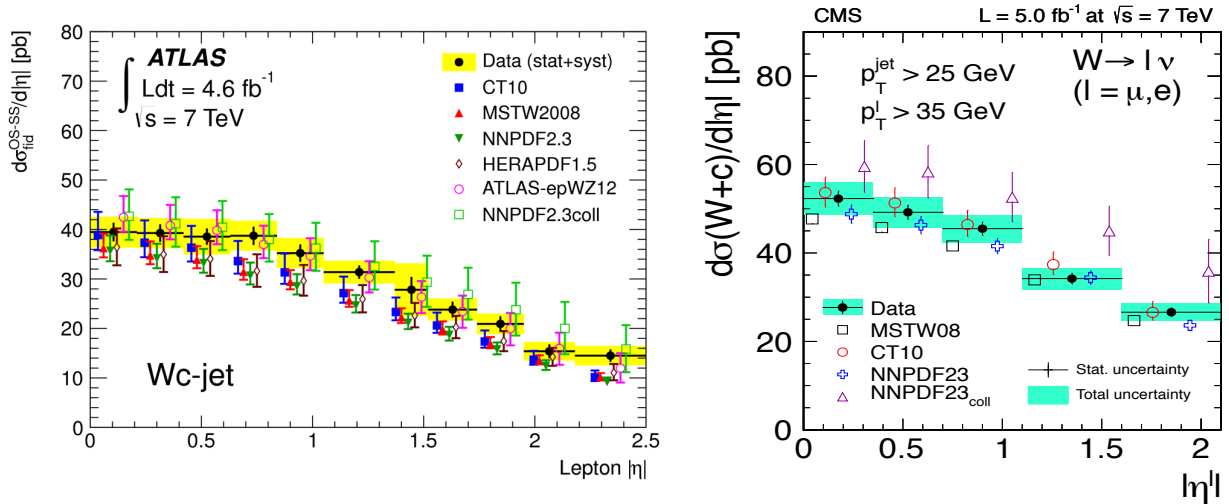


Figure 6 – The lepton pseudorapidity distribution for the  $W$ +charm jet cross section from ATLAS (left) and the  $W$ +charm cross section at CMS (right).

be lower than that expected by the CMS cross section. However, it should be noted that in both cases, the treatment of the charm-to-jet fragmentation is treated differently, with CMS extrapolating back to the parton level.

### 7.1 QCD fits including heavy electroweak boson production

When including the electroweak boson data in a QCD fit, both collaborations allow the parameters for the strange quark density to vary independently, producing a 15 parameter fit, in contrast to the 13 parameter fit with a constrained strange quark density used for the fits to the jet data.

For the Electroweak boson cross sections, APPLgrid is used interfaced to MCFM<sup>36</sup>, and using an NNLO K-factor obtained from FEWZ<sup>37</sup> in the case of the ATLAS fit to 2010 inclusive  $Z$  and  $W$  asymmetry data<sup>38</sup>, and at NLO and for the CMS fit<sup>32</sup>, this time to the 2011  $W$  asymmetry data together the  $W + c$ , with the  $W + c$  data extrapolated back to the total charm jet cross section at parton level.

In addition, the new ATLAS measurement includes an *eigenvector* fit to the 2011 ATLAS  $W + c$  data using the HERAPDF1.5 eigenvector set. Here, the data is fit at true hadron level by fitting a linear combination of the HERAPDF eigenvector sets with the constraint on the strangeness suppression factor released and allowed to vary in the fit.

The distribution of the strangeness ratio,  $r_s = (s + \bar{s})/2\bar{d}$  from the ATLAS and CMS fits can be seen in Fig. 7. The left plot shows the comparison of the ATLAS NNLO fit, with the free strangeness distribution, compared to the HERAPDF1.5 fit, and the ATLAS NLO eigenvector fit to the  $W + c$ . In both the ATLAS fits, a value of  $r_s$  close to 1 is obtained. On the right, the ATLAS fits are compared to the value obtained from the NLO QCD fit to the combined  $W$  asymmetry, and  $W + c$  data from CMS. The CMS fit also suggests an enhanced strange contribution with respect to the HERPDF at low- $x$ , although not as large as that predicted by the ATLAS fit, being somewhat lower at higher  $x$ .

These data on  $W$  production in conjunction with a charm quark from both ATLAS and CMS are quite recent and potentially extremely promising and tools are still being developed to more properly include them in a QCD fit, which should shed more light on the strange quark density.

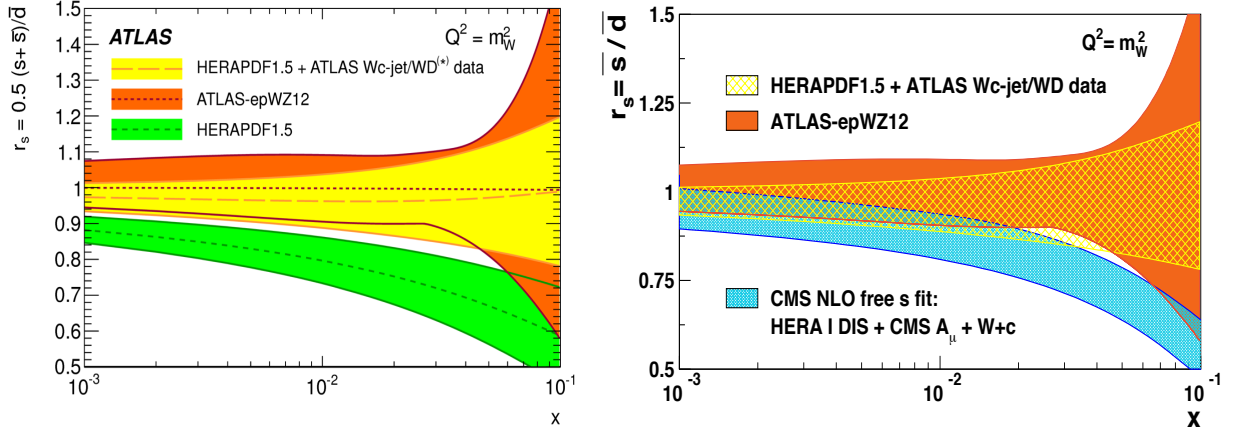


Figure 7 – The resulting  $r_s$  parameter from the ATLAS NNLO, and eigenvector fits (left) and both the ATLAS fits and the full CMS NLO fit to the  $W$  asymmetry and  $W + c$  CMS data (right).

## 8 Outlook

Both ATLAS and CMS have a large, and growing portfolio of precision measurements that have the potential to significantly constrain the parton distributions in the proton, a small selection of which have been discussed here. Higher luminosity data is already available and are being analysed with a view to reducing both the statistical and systematic uncertainties of the measurements.

For some of the data, the potential is limited only by the theoretical uncertainty, or the available fast convolution grid technology from fastNLO or APPLgrid. For some processes, such as jet production, and the  $W$ +charm production, calculations are available only at NLO. In these cases, theoretical uncertainties are often comparable to, or larger, than those from the data. However, these new precise data are only now becoming available, and developments in both the theoretical calculations and in the fast grid technologies over the last few years mean that much of this can, in principle, now be used in QCD fits - something that would not have been possible even a few years ago.

The journey towards better understanding of the parton distributions within the proton using the LHC data has only just begun, but the significant promise of the new data mean that it will be a very interesting time ahead.

## 9 Acknowledgements

The author would like to thank the University of Sussex for funding to attend the workshop and the workshop Organising Committee for a most interesting workshop.

## References

1. L. Evans and P. Bryant, LHC Machine, Tech. Rep. JINST 3:S08001 (2008).
2. The ATLAS Collaboration; JINST 3:S08003 (2008).
3. The CMS Collaboration; JINST 3:S08004 (2008).
4. R. G. Roberts, ‘The Structure of the Proton’, Cambridge University Press (1990).
5. D. Britzger et al; arXiv:1208.3641 [hep-ph] (2012).
6. T. Carli *et al*; Eur. Phys. J. **C66** (2010) 503.
7. H.-L. Lai *et al*; Phys. Rev. **D82** (2010) 074024, arXiv:hep-ph/1007.2241.

8. A. Martin, W. Stirling, R. Thorne, and G. Watt; Eur. Phys. J. **C63** (2009) 189285, arXiv:hep-ph/0901.0002.
9. S. Alekhin, J. Bluemlein, and S.-O. Moch; PoS LL 2012 (2012) 016, arXiv:hep-ph/1302.1516.
10. The H1 and ZEUS Collaborations; H1-prelim-10-142, ZEUS-prel-10-018. [http://www.desy.de/h1zeus/combined\\_results/index.php?do=proton\\_structure](http://www.desy.de/h1zeus/combined_results/index.php?do=proton_structure).
11. G. Watt; JHEP 1109:069 (2011), arXiv:hep-ph/1106.5788.
12. The ATLAS Collaboration; Submitted to JHEP (2013), arXiv:hep-ex/1312.3524.
13. The CMS Collaboration; Phys. Rev. **D87** (2012) 12002.
14. The ATLAS Collaboration; Eur. Phys. J. **C73** (2013) 2509.
15. J. Currie *et al*; (2013) arXiv:hep-ph/1310.3993.
16. The CMS Collaboration; CMS-PAS-SMP-12-028, CERN (2013).
17. The CMS Collaboration; Phys. Rev. **D87** (2013) 112002.
18. The ATLAS Collaboration; ATLAS-CONF-2013-099, CERN (2013).
19. The CMS Collaboration; Phys. Lett. **B728** (2013) 496, arXiv:hep-ex/1307.1907.
20. The CMS Collaboration; Eur. Phys. J. **C73** (2013) 2604.
21. The CMS Collaboration; CMS-PAS-SMP-12-027, CERN (2013).
22. The H1 Collaboration; Eur. Phys. J. C 65 (2010) 363, arXiv:hep-ex/0904.3870.
23. The H1 Collaboration; Eur. Phys. J. C 67 (2010) 1, arXiv:hep-ex/0911.5678.
24. The ZEUS Collaboration; Nucl. Phys. B 864 (2012) 1, arXiv:hep-ex/1205.6153.
25. The CDF Collaboration; Phys. Rev. Lett. 88 (2002) 042001, arXiv:hep-ex/0108034.
26. The D0 Collaboration; Phys. Rev. D 80 (2009) 111107, arXiv:hep-ex/0911.2710.
27. D0 Collaboration, Measurement of angular correlations of jets at determination of the strong coupling at high momentum transfers, Phys. Lett. B 718 (2012) 56, arXiv:hep-ex/1207.4957.
28. The ATLAS Collaboration; ATL-PHYS-PUB-2013-018, CERN (2013).
29. The ATLAS Collaboration; (2013) arXiv:hep-ex/1311.1440.
30. The ATLAS Collaboration; Phys. Lett. **B725** (2013) 223-242.
31. The CMS Collaboration; JHEP 12 (2013) 030.
32. The CMS Collaboration; (2013) arXiv:hep-ex/1312.6283v2.
33. The ATLAS Collaboration; (2014) arXiv:hep-ex/1402.6263v1.
34. The CMS Collaboration; arXiv:1310.1138 [hep-ex] (2013).
35. R. Ball *et al*; Nucl. Phys. **B867** (2013) 244289, (2012) arXiv:hep-ph/1207.1303.
36. J. M. Campbell and R. K. Ellis; Nucl. Phys. Proc. Suppl. 205-206, 10 (2010).
37. C. Anastasiou, *et al*; Phys. Rev. **D69** (2004) 094008.
38. The ATLAS Collaboration; Phys. Rev. Lett. 109 (2012) 012001.